# Complement-Inhibiting Iridoids from *Morinda morindoides*

Kanyanga Cimanga, Nina Hermans, Sandra Apers, Sabine Van Miert, Hilde Van den Heuvel, Magda Claeys, Luc Pieters,* and Arnold Vlietinck

*Department of Pharmaceutical Sciences, University of Antwerp, Universiteitsplein 1, B-2610 Antwerp, Belgium*

*Received May 13, 2002*

*Morinda morindoides* (Baker) Milne-Redhead (syn. *Gaertnera morindoides* Bak.) is one of the most popular medicinal plants in the Democratic Republic of Congo. In relation to its traditional use against rheumatic pains, fractionation of both the EtOAc- and the *n*-BuOH-soluble fraction of the 80% MeOH extract of the leaves, guided by the anticomplementary activity on the classical activation pathway, yielded eight novel iridoids (**1**−**8**), all containing a spirolactone functionality. Their structure was elucidated using spectroscopic methods. Gaertneroside **1**, acetylgaertneroside **2**, and gaertneric acid **5** were found to inhibit the activation of the classical pathway of the complement system, with $IC_{50}$ values between 58 and 69 $\mu$M. In addition to the biologically active flavonoids reported before from the same plant, these complement-inhibiting iridoids may contribute at least in part to the traditional use against rheumatic pains.

*Morinda morindoides* (Baker) Milne-Redhead (Rubiaceae) (syn. *Gaertnera morindoides* Bak.), commonly called Nkongabululu, Kongobololo, or Nkama mesu in the Democratic Republic of Congo, is one of the most popular medicinal plants used in this African country. A decoction of the leaves, a typical preparation in traditional medicine, is used for the treatment of various diseases such as fever (including fever caused by malaria), amoebiasis, haemorrhoids, intestinal worms, and gonorrhea, as an antirheumatic agent, and as a tonic.[1] The traditional use of the leaves of this plant is also described in other African countries.[2] With respect to the use of the leaves of *M. morindoides* for the treatment of rheumatic pains, a bioassay-guided fractionation of both the EtOAc- and *n*-BuOH-soluble fractions of the 80% MeOH extract of the leaves has resulted in the isolation and structure elucidation of a series of flavonoids[3] for which anticomplementary,[4,5] radical scavenging, and xanthine oxidase inhibitory activities were documented.[6] Since the complement system is one of the major effector pathways in the process of inflammation, inhibitors of complement activation are potentially useful in the treatment of inflammatory diseases. In this study, the isolation, the structure elucidation, and the anticomplementary activity of a series of iridoids (**1**−**8**) from the leaves of *M. morindoides* are reported.

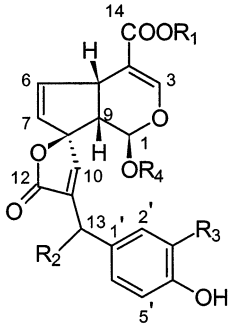

| | $R_1$ | $R_2$ | $R_3$ | $R_4$ |
|---|---|---|---|---|
| **1** | Me | OH | H | glucosyl |
| **2** | Me | OH | H | 6-acetyl-glucosyl |
| **3** | Me | =O | H | glucosyl |
| **4** | Me | =O | OMe | glucosyl |
| **5** | H | OH | H | glucosyl |
| **6** | Me | OH | OMe | glucosyl |

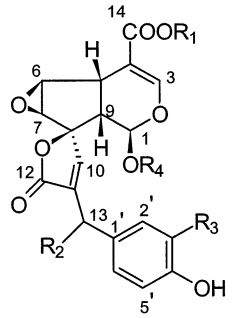

| | $R_1$ | $R_2$ | $R_3$ | $R_4$ |
|---|---|---|---|---|
| **7** | Me | OH | H | glucosyl |
| **8** | Me | OH | OMe | glucosyl |

## Results and Discussion

The 80% MeOH extract of leaves of *M. morindoides* was dissolved in $H_2O$ after evaporation to dryness and successively partitioned against $CHCl_3$, EtOAc, and *n*-BuOH. Both the EtOAc and the *n*-BuOH extract inhibited the classical activation pathway of the complement system. The EtOAc fraction showed an $IC_{50}$ value of 55.7 ± 9.5 $\mu$g/mL, while the $IC_{50}$ value for the *n*-BuOH fraction was 89.1 ± 6.1 $\mu$g/mL. In addition to the anticomplementary flavonoid glycosides reported before,[4,5] a series of iridoids was isolated from these active fractions: The EtOAc and the *n*-BuOH extracts yielded eight novel iridoids (**1**−**8**). Their structures were elucidated using spectroscopic methods.

The $^1$H and $^{13}$C NMR spectra of compound **1** showed the characteristic signals of a glucosidic moiety, with an anomeric proton at $\delta$ 4.67 (H-1″, d, $J$ = 7.9 Hz), correlated in the HSQC spectrum (showing one-bond C−H correlations) to an anomeric carbon at $\delta$ 100.57 (C-1″). Also present were the signals diagnostic of a *para*-substituted aromatic ring with a typical AA′BB′ coupling pattern in the $^1$H NMR ($\delta$ 6.78 and 7.28, 2H each, d, $J$ = 8.6 Hz), correlated to two signals with approximately double intensity at $\delta$ 116.30 and 129.67, respectively. The presence of a CH signal in the $^{13}$C NMR spectrum, relatively downfield at $\delta$ 152.56 (C-3), correlated in the HSQC spectrum with

* To whom correspondence should be addressed. Tel and fax: (32) 3-820 27 09. E-mail: luc.pieters@ua.ac.be.

10.1021/np020215h CCC: $25.00 
Published on Web 12/20/2002

**Table 1.** Complete $^1$H and $^{13}$C NMR Assignments ($CD_3OD$, 400 and 100 MHz, respectively), $^1$H−$^1$H, and Long-Range $^1$H−$^{13}$C Correlations of Gaertneroside (**1**)

| carbon no. | $^{13}$C NMR $\delta$ (ppm) | $^1$H NMR $\delta$ (ppm), mult., $J$ (Hz) | $^1$H−$^1$H correlations[a] | $^1$H−$^{13}$C long-range correlations[b] (C→H) |
|---|---|---|---|---|
| 1 | 94.50 | 5.14, d, 4.9 | H-9 | H-3, H-9, H-1″ |
| 3 | 152.56 | 7.51, d, 1.6 | H-5 | H-1 |
| 4 | 110.92 | | | H-3, H-5, H-9 |
| 5 | 40.39 | 3.90, m | H-3, H-6, H-7, H-9 | H-1, H-3, H-6, H-7, H-9 |
| 6 | 141.63 | 6.46, dd, 5.6, 2.5 | H-5, H-7 | H-5, H-7, H-9 |
| 7 | 129.99 | 5.56, dd, 5.6, 2.2 | H-5, H-6 | H-6 |
| 8 | 98.09 | | | H-1, H-6, H-7, H-9, H-10 |
| 9 | 50.84 | 2.90, dd, 7.6, 4.9 | H-1, H-5 | H-6, H-7 |
| 10 | 150.15 | 7.45, d, 1.3 | H-13 | H-13 |
| 11 | 137.92 | | | H-10, H-13 |
| 12 | 172.42 | | | H-10, H-13 |
| 13 | 69.94 | 5.36, d, 1.3 | H-10 | H-10, H-3′,5′ |
| 14 | 168.48 | | | H-3, -OMe |
| 1′ | 133.32 | | | H-13, H-2′,6′ |
| 2′,6′ | 116.30 | 6.78, d, 8.6 | H-3′,5′ | H-2′, H-6′ |
| 3′,5′ | 129.67 | 7.28, d, 8.6 | H-2′,6′ | H-13, H-3′,5′ |
| 4′ | 158.57 | | | H-2′,6′, H-3′,5′ |
| 1″ | 100.57 | 4.67, d, 7.9 | H-2″ | H-1, H-2″ |
| 2″ | 74.51 | 3.21, m | H-1″,H-3″ | H-3″ or H-4″ |
| 3″ | 77.91 | 3.38, m | H-2″ | H-2″ |
| 4″ | 70.94 | 3.38, m | H-5″ | H-3″ |
| 5″ | 78.41 | 3.25, m | H-4″, H-6″a, H-6″b | H-3″ or H-4″ |
| 6″a | 62.22 | 3.79, dd, 12.2, 2.2 | H-5″, H-6″a | |
| 6″b | | 3.68, dd, 12.2, 4.9 | H-5″, H-6″a | |
| -COO*Me* (R1) | 51.99 | 3.75, s | | |

[a] Observed in a $^1$H,$^1$H-DQF COSY experiment. [b] Observed in a HMBC experiment optimized for a long-range coupling constant $J_{C,H}$ of 8.3 Hz.

**Table 2.** ES-MS and ES-MS/CID/MS Data Obtained for Compounds **1**−**8**

| | | ES-MS | | | ES-MS/CID/MS[a] $[M + Na]^+$ | |
|---|---|---|---|---|---|---|
| compound | MW | $[M - H]^-$, *m/z* | $[M + Na]^+$, *m/z* | $[2M + Na]^+$, *m/z* | low-energy, *m/z* | high-energy, *m/z* |
| **1** | 548 | 547 | 571 | 1119 | 203, **329**, 373, 391, 527 | 203, 231, 304, 329, **512** |
| **2** | 590 | 589 | 613 | 1203 | **245**, 329, 351, 373, 391 | **245**, 273, 329, 520, 554 |
| **3** | 546 | 545 | 569 | 1015 | 121, 203, 345, **389**, 407 | 302, 389, 390, **432**, 510 |
| **4** | 576 | 575 | 599 | 1175 | 151, 203, 375, **419** | 332, 419, **432**, 540, 584 |
| **5** | 534 | 533 | 557 | 1091 | 203,**315**, 359, 377, 513 | **203**, 304, 315, 377, 464, 512* |
| **6** | 578 | 577 | 601 | 1179 | 203, **359**, 381, 421, 557 | 203, 231, 334, 359, **542**, 478* |
| **7** | 564 | 563 | 587 | 1151 | *b* | 185, 231, 269, 453, **528**, 494* |
| **8** | 594 | 593 | 617 | 1181, $[M + M(\mathbf{7}) + Na]^+$ | *b* | 185, 231, 299, 350, **558** |

[a] The five most abundant product ions in the CID spectra are listed. For compound **4** only four product ions were formed in low-energy CID. The most abundant ion is highlighted in bold. Minor diagnostic ions discussed in the text are also included and marked with an asterisk. [b] The $[M + Na]^+$ ion of the epoxides **7** and **8** did not fragment in low-energy CID.

H-3 at $\delta$ 7.51 (H-3, d, $J$ = 1.6 Hz), suggested an iridoid-like structure. This hypothesis was supported by a $^1$H NMR signal at $\delta$ 5.14 (H-1, d, $J$ = 4.9 Hz), corresponding to a CH signal at $\delta$ 94.50 in the $^{13}$C NMR (C-1). Moreover, C-1 was correlated to H-1″ and H-3 in the HMBC spectrum (showing multiple-bond C−H correlations), and C-1″ was correlated to H-1. The presence in the $^{13}$C NMR spectrum of a carbonyl group at $\delta$ 172.42 (C-12), a CH group at $\delta$ 150.15 (C-10), and quaternary carbons at $\delta$ 98.09 (C-8) and 133.32 (C-1′) indicated that compound **1** belonged to the relatively rare group of plumeria iridoids containing a characteristic spirolactone functionality.[7] Comparison with published NMR assignments revealed a good similarity with plumieride,[8] but compound **1** contained a *para*-substituted aromatic moiety. Detailed analysis of the NMR spectra, especially the HMBC spectrum, revealed that in **1** a 4′-hydroxyphenyl moiety was attached to an oxygenated carbon (C-13, $\delta$ 69.94 in $^{13}$C NMR, $\delta$ 5.36 in $^1$H NMR), being a substituent of the spirolactone ring. The two-dimensional NMR spectra allowed to fully establish the structure of **1** as a novel iridoid of the plumeria type, for which the name gaertneroside was adopted. $^1$H and $^{13}$C NMR assignments, as well as $^1$H−$^1$H, one-bond $^1$H−$^{13}$C, and long-range $^1$H−$^{13}$C correlations, observed in a double quantum filtered COSY, a HSQC, and a HMBC experiment, respectively, are listed in Table 1. On the basis of the $^1$H and $^{13}$C NMR assignments, and their similarity with those reported for plumieride, the same relative configuration was adopted for gaertneroside (**1**). However, the stereochemistry at C-13 of gaertneroside, which is not part of the rigid skeleton of the molecule, could not be assigned. The structure of gaertneroside (**1**) was also confirmed by ES-MS and ES-MS/CID/MS (Table 2) and accurate mass measurement of the $[M - H]^-$ ion. The first-order ES spectra showed $[M + Na]^+$ and $[2M + Na]^+$ signals at *m/z* 571 and 1119, respectively, in the positive ion mode, and a $[M - H]^-$ signal at *m/z* 547, in the negative ion mode, consistent with a MW of 548. The low-energy $[M + Na]^+$ CID spectrum revealed a neutral loss of 180 u (*m/z* 391), corresponding to the loss of a hexose, and an ion at *m/z* 203, due to $[\text{hexose} + Na]^+$, features which can both be considered as characteristic of an iridoid 1-*O*-glucoside. In addition, ions were present at *m/z* 527 (loss of $CO_2$), *m/z* 373 (combined loss of glucose and $H_2O$), and *m/z* 329 (combined loss of glucose, $H_2O$, and $CO_2$), which can all be rationalized on the basis of the proposed structure.

**Table 3.** $^1$H NMR Assignments of Compounds **2**−**8** ($CD_3OD$, 400 MHz)

| | $\delta_H$ (ppm), mult., *J* (Hz) | | | | | | |
|---|---|---|---|---|---|---|---|
| carbon no. | **2** | **3** | **4** | **5** | **6** | **7** | **8** |
| 1 | 4.99, d, 4.3 | 5.40, d, 5.5 | 5.48, d, 4.9 | 5.04, d, 4.9 | 5.13, d, 3.7 | 5.05, br s | 5.04, br s |
| 3 | 7.52, d, 1.5 | 7.50, br s | 7.50, br s | 7.49, d, 1.0 | 7.50, d, 1.5 | 7.60, br s | 7.61, br s |
| 5 | 3.88, m | 3.98, m | 3.98, m | 3.90, m | 3.88, m | 3.45, br d, 8.3 | 3.45, br d, 8.3 |
| 6 | 6.48, dd, 5.6, 2.5 | 6.54, dd, 5.6, 2.5 | 6.54, dd, 5.6, 2.5 | 6.56, dd, 5.6, 2.4 | 6.47, dd, 5.6, 2.6 | 3.42, br d, 2.5 | 3.42, d, 2.5 |
| 7 | 5.59, dd, 5.6, 2.0 | 5.69, dd, 5.6, 2.1 | 5.67, dd, 5.6, 2.1 | 5.47, dd, 5.6, 2.1 | 5.56, dd, 5.6, 1.9 | 4.05, br d, 2.5 | 4.05, d, 2.5 |
| 9 | 2.93, dd, 7.6, 4.3 | 3.05, m | 3.05, m | 2.83, dd, 7.5, 4.9 | 2.97, dd, 7.9, 3.7 | 2.74, br d, 8.3 | 2.74, br d, 8.3 |
| 10 | 7.35, d, 1.3 | 7.85, br s | 7.85, br s | 7.25, br s | 7.33, br s | 7.15, d, 1.4 | 7.19, d, 1.3 |
| 13 | 5.36, d, 1.1 | | | 5.35, br s | 5.37, d, 2.1 | 5.37, d, 1.4 | 5.37, d, 1.4 |
| 2′ | 6.80, d, 8.6 | 6.88, d, 8.8 | 7.50, m | 6.78, d, 8.5 | 7.01, d, 1.9 | 6.76, d, 8.5 | 6.97, d, 1.9 |
| 3′ | 7.28, d, 8.6 | 7.83, d, 8.8 | | 7.28, d, 8.5 | | 7.23, d, 8.5 | |
| 5′ | 7.28, d, 8.6 | 7.83, d, 8.8 | 6.88, d, 8.4 | 7.0.28, d, 8.5 | 6.79, d, 8.1 | 7.23, d, 8.5 | 6.76, d, 8.1 |
| 6′ | 6.80, d, 8.6 | 6.88, d, 8.8 | 7.50, m | 6.78, d, 8.5 | 6.90, dd, 8.1, 1.9 | 6.76, d, 8.5 | 6.88, dd, 8.1, 1.9 |
| 1″ | 4.63, d, 8.0 | 4.68, d, 7.9 | 4.65, 7.9 | 4.67, d, 7.9 | 4.58, d, 7.9 | 4.51, d, 7.9 | 4.45, d, 7.9 |
| 2″ | 3.18, dd, 9.1, 8.0 | 3.15, m | 3.15, m | 3.2−3.4, m | 3.15, m | 3.11, dd, 7.9, 8.0 | 3.11, dd, 7.9, 8.0 |
| 3″ | 3.39, m | 3.32, m | 3.32, m | 3.2−3.4, m | 3.35, m | 3.30, m[a] | 3.30, m[a] |
| 4″ | 3.30, m[a] | 3.30, m[a] | 3.30, m[a] | 3.2−3.4, m | 3.35, m | 3.35, m | 3.35, m |
| 5″ | 3.47, m | 3.25, m | 3.25, m | 3.2−3.4, m | 3.25, m | 3.21, m | 3.21, m |
| 6″a | 4.24, m | 3.79, dd, 12.2, 2.2 | 3.79, dd, 12.2, 2.2 | 3.77, dd, 12.1, 2.0 | 3.65−3.70, m | 3.70, m | 3.70, m |
| b | 4.24, m | 3.68, dd, 12.2, 4.9 | 3.68, dd, 12.2, 4.9 | 3.69, dd, 12.1, 4.3 | 3.65−3.70, m | 3.70, m | 3.70, m |
| −COOMe ($R_1$) | 3.76, s | 3.74, s | 3.74, s | | 3.75, s | 3.78, s | 3.78, s |
| −OCOMe ($R_4$) | 1.87, s | | | | | | |
| −OMe ($R_3$) | | | 3.92, s | | 3.89, s | | |

[a] Masked by solvent.

**Table 4.** $^{13}$C NMR Assignments of Compounds **2**−**8** ($CD_3OD$, 100 MHz)

| carbon | $\delta_C$ (ppm) | | | | | | |
|---|---|---|---|---|---|---|---|
| no. | **2** | **3** | **4** | **5** | **6** | **7** | **8** |
| 1 | 94.43 | 94.32 | 94.05 | 94.04 | 93.79 | 92.49 | 92.34 |
| 3 | 152.51 | 152.74 | 152.48 | 148.13 | 152.09 | 153.88 | 153.17 |
| 4 | 111.10 | 110.86 | 111.09 | 116.29 | 111.43 | 108.03 | 108.14 |
| 5 | 39.93 | 40.93 | 40.62 | 51.25 | 39.67 | 32.85 | 32.85 |
| 6 | 141.42 | 142.67 | 142.35 | 143.40 | 140.86 | 58.92 | 58.92 |
| 7 | 130.09 | 128.98 | 129.12 | 128.66 | 130.24 | 57.89 | 57.85 |
| 8 | 97.95 | 97.84 | 97.79 | 98.74 | 97.91 | 92.70 | 92.70 |
| 9 | 51.01 | 51.47 | 51.40 | 41.82 | 50.81 | 43.91 | 43.92 |
| 10 | 150.10 | 159.29 | 159.00 | 151.09 | 149.78 | 146.89 | 146.65 |
| 11 | 138.25 | 131.65 | 131.62 | 137.43 | 138.21 | 140.72 | 140.76 |
| 12 | 172.47 | 169.96 | 169.96 | 172.83 | 172.38 | 171.58 | 171.56 |
| 13 | 69.77 | 188.27 | 188.11 | 69.94 | 70.00 | 69.97 | 70.24 |
| 14 | 168.42 | 168.36 | 168.32 | 180.60 | 168.38 | 167.97 | 167.94 |
| 1′ | 133.41 | n.a.[a] | 128.74 | 133.36 | 133.93 | 132.97 | 133.55 |
| 2′ | 116.41 | 116.37 | 112.63 | 116.29 | 111.65 | 116.19 | 111.28 |
| 3′ | 129.59 | 133.61 | 149.75 | 129.71 | 149.06 | 129.56 | 149.13 |
| 4′ | 158.62 | 165.50 | 155.50 | 158.55 | 147.63 | 158.60 | 147.71 |
| 5′ | 129.59 | 133.61 | 116.91 | 129.71 | 116.07 | 129.56 | 115.84 |
| 6′ | 116.41 | 116.37 | 127.26 | 116.29 | 121.17 | 116.19 | 121.42 |
| 1″ | 100.62 | 100.18 | 100.02 | 100.51 | 100.08 | 99.63 | 99.46 |
| 2″ | 74.29 | 74.59 | 74.59 | 74.60 | 74.41 | 74.34 | 74.34 |
| 3″ | 77.69 | 77.85 | 77.75 | 77.88 | 77.86 | 77.84 | 77.84 |
| 4″ | 71.50 | 71.65 | 71.65 | 70.98 | 70.83 | 70.76 | 70.66 |
| 5″ | 75.74 | 78.70 | 78.70 | 78.29 | 78.26 | 78.10 | 78.05 |
| 6″ | 64.69 | 62.87 | 62.87 | 62.23 | 62.05 | 61.81 | 61.73 |
| −COO*Me* ($R_1$) | 52.02 | 51.97 | 51.97 | | 51.94 | 52.03 | 52.03 |
| −OCOMe ($R_4$) | 172.98 | | | | | | |
| −OCO*Me* ($R_4$) | 20.70 | | | | | | |
| −OMe ($R_3$) | | | 56.47 | | 56.52 | | 56.44 |

[a] Not assigned.

Compound **2** produced NMR spectra very similar to those of gaertneroside (**1**), but the presence of an additional acetyl group was evident from $^{13}$C NMR signals at $\delta$ 172.98 (carbonyl group) and 20.70 (methyl group), the latter one corresponding to an additional singlet in $^1$H NMR at $\delta$ 1.87 (Tables 3 and 4). A multiple-bond correlation was observed in the HMBC spectrum between the acetyl carbonyl group and H-6″ at $\delta$ 4.24 in $^1$H NMR, indicating acetylation at this position. This was also evident from the downfield shift of C-6″ from $\delta$ 62.22 in **1** to 64.69 in **2**. The presence of an additional acetyl group in the 1-*O*-glucosyl substituent was confirmed by ES-MS and ES-MS/CID/MS (Table 2) and accurate mass measurement of the $[M - H]^-$ ion. The low-energy $[M + Na]^+$ CID spectrum revealed a neutral loss of 222 u, corresponding to the loss of an acetylated hexose (*m*/*z* 391), and an ion at *m*/*z* 245, due to [Ac − hexose + $Na]^+$. Hence, the structure of compound **2** could be established unequivocally as 6″-acetylgaertneroside, a novel iridoid. Since no acetic acid was employed during the isolation, obviously this compound cannot be considered as an artifact.

Compound **3** was also very similar to gaertneroside (**1**), but in the $^{13}$C NMR spectrum the CH signal at $\delta$ 69.94 (C-13) was missing, as well as the corresponding $^1$H NMR signal at $\delta$ 5.36 (H-13) (Tables 3 and 4). On the other hand, an additional carbonyl functionality was observed at $\delta$ 188.27 in the $^{13}$C NMR, which showed long-range correlations in the HMBC spectrum to H-10 ($\delta$ 7.85) of the spirolactone ring and to H-2′/H-6′ ($\delta$ 6.88) of the aromatic moiety. Therefore, the structure of compound **3** was established as the 13-keto analogue of gaertneroside (**1**), a new compound for which the name dehydrogaertneroside was adopted. The structure of compound **3** was further supported by ES-MS and ES-MS/CID/MS (Table 2) and accurate mass measurement of the $[M - H]^-$ ion. The low-energy $[M + Na]^+$ CID spectrum revealed an ion at *m*/*z* 121, corresponding to a hydroxybenzoyl cation $[HO - \Phi - C(=O)]^+$ and thus consistent with the presence of a *p*-hydroxybenzoyl group. Furthermore, the ions typical of an iridoid 1-*O*-glucoside were also noted at *m*/*z* 389 (loss of a hexose) and at *m*/*z* 203 [hexose + $Na]^+$.

The carbonyl group at C-13 present in compound **3** was also found for compound **4**, a structural feature that was revealed from the $^{13}$C NMR spectrum showing a signal at $\delta$ 188.11 (Tables 3 and 4). An additional methoxyl substituent was indicated ($\delta$ 56.47 in $^{13}$C NMR, and a singlet at $\delta$ 3.92 in $^1$H NMR), but the typical signals of the *para*-substituted aromatic moiety were missing. Instead, the $^1$H NMR spectrum showed the typical coupling pattern of a 1,3,4-trisubstituted phenyl group instead. Detailed analysis of the one- and two-dimensional NMR spectra indicated the presence of a 3′-methoxy-4′-hydroxyphenyl substituent at C-13, instead of a 4′-hydroxyphenyl group found in compound **3**. The structure of compound **4** was established

as the 3′-methoxy derivative of dehydrogaertneroside (**3**), a new compound for which the name dehydromethoxygaertneroside was adopted. The structure of compound **4** was further confirmed by ES-MS and ES-MS/CID/MS (Table 2) and accurate mass measurement of the $[M - H]^-$ ion. The low-energy $[M + Na]^+$ CID spectrum showed a diagnostic ion at *m/z* 151, consistent with the presence of a 3′-methoxy-4′-hydroxybenzoyl group. As expected, the ions typical of an iridoid 1-*O*-glucoside were also noted at *m/z* 419 (loss of a hexose) and at *m/z* 203 [hexose + $Na]^+$.

In the $^1$H and $^{13}$C NMR spectra of compound **5** the signals due to the characteristic methoxycarbonyl group (COO*Me*), occurring, for example, at $\delta$ 3.75 in the $^1$H NMR and at $\delta$ 51.99 in $^{13}$C NMR spectrum of **1**, were missing, which suggested this compound to be the unesterified analogue of **1** (Tables 3 and 4). This hypothesis was supported by ES-MS and ES-MS/CID/MS (Table 2) and accurate mass measurement of the $[M - H]^-$ ion. The presence of a carboxyl group in compound **5** (instead of a methylcarboxyl group in compound **1**) was evident from the high-energy $[M + Na]^+$ CID spectrum, which revealed an ion at *m/z* 512 corresponding to the loss of a carboxyl (•COOH) radical (instead of •$COOCH_3$ loss in the case of compound **1**). The name gaertneric acid was adopted for compound **5**.

The $^1$H and $^{13}$C NMR spectra of compound **6** again were very similar to those of compound **1**, but here the typical signals of the 4′-hydroxyphenyl moiety were absent (Tables 3 and 4). Instead, the same 3′-methoxy-4′-hydroxyphenyl group as in compound **4** was present. In this way the structure of **6** could be established as the 3′-methoxy derivative of gaertneroside (**1**), for which the name methoxygaertneroside was adopted. The low-energy $[M + Na]^+$ CID spectrum was very similar to that of compound **1**, showing the appropriate mass shifts for an additional methoxyl group (Table 2). The presence of a 3′-methoxy-4′-hydroxyphenyl group (instead of a 4′-hydroxyphenyl group in compound **1**) was evident from the high-energy $[M + Na]^+$ CID spectrum, which revealed a minor ion at *m/z* 478 formed by the loss of the corresponding radical (123 u).

In the $^1$H and $^{13}$C NMR spectra of compound **7**, the characteristic signals due to the 6,7-double bond ($\delta$ 6.46 (dd) and 5.56 (dd) in $^1$H NMR, and $\delta$ 141.63 and 129.99 in $^{13}$C NMR, for compound **1**) had disappeared (Tables 3 and 4). However, new signals were observed in the $^1$H NMR at $\delta$ 3.42 (br d, $J = 2.5$ Hz), corresponding to a CH signal at $\delta$ 58.92 in the $^{13}$C NMR (C-6), and at $\delta$ 4.05 (br d, $J = 2.5$ Hz), corresponding to a CH signal at $\delta$ 57.89 in the $^{13}$C NMR (C-7), which indicated the presence of a 6,7-epoxide. It is worth mentioning that also in *Allamanda neriifolia* the iridoid plumieride was accompanied by its 6,7-epoxide plumiepoxide. The fact that no coupling was observed between H-5 and H-6 indicated a $\beta$-orientation of the epoxide ring, as discussed before for plumiepoxide.[12] The name epoxygaertneroside was adopted for compound **7**. The presence of a 3′-methoxy-4′-hydroxyphenyl group was evident from the high-energy CID spectrum (Table 2), revealing an ion at *m/z* 494 due to the loss of the corresponding radical (123 u). Ions typical of an iridoid 1-*O*-glucoside were noted at *m/z* 453, 231, and 185, which can be explained by cross-ring or glycosidic cleavages. In addition, an abundant ion was present at *m/z* 528 due to the loss of the methylcarboxyl group (45 u).

Compound **8** could only be isolated in trace amounts (<1 mg). However, its complete $^1$H and $^{13}$C NMR spectral data could easily be deduced from the spectra of the mixture of **7** and **8** before separation (Tables 3 and 4). Compound **8** showed the same characteristic signals of a 6,7-$\beta$-epoxide functionality already observed in the NMR spectra of **7**, but instead of a 4′-hydroxyphenyl group, it contained a 3′-methoxy-4′-hydroxyphenyl moiety. Therefore, compound **8** was a 3′-methoxy derivative of **7**, for which the name epoxymethoxygaertneroside was adopted. The MW of 594 was inferred from the first-order ES spectra, showing, in the negative ion mode, a $[M - H]^-$ signal at *m/z* 593 and, in the positive ion mode, a $[M + Na]^+$ signal at *m/z* 617 and also an ion at *m/z* 1181 due to complexation with compound **7**, a major component of the mixture. The high-energy CID spectrum was very similar to that of compound **7**, but showed the appropriate mass shifts for an additional methoxyl group (Table 2).

The iridoids **1**−**8** are structurally related to the plumeria iridoids, a relatively rare group of iridoids containing a spirolactone ring, which are found mainly in the Apocynaceae.[7] In the Rubiaceae, more specifically in the genus *Morinda*, only a few iridoids with this typical functionality have been identified, such as oruwacin from *Morinda lucida*,[9] citrifolinoside A from *Morinda citrifolia*,[10] and yopaaosides A and B from *Morinda coreia*.[11]

Gaertneroside **1**, acetylgaertneroside **2**, and gaertneric acid **5** were found to inhibit the activation of the classical pathway of the complement system. Gaertneroside **1**, acetylgaertneroside **2**, and gaertneric acid **5** showed $IC_{50}$ values of 58 ± 6 , 71 ± 6, and 69 ± 24 $\mu$M, respectively. Compounds **3**, **4** ($IC_{50}$ > 400 $\mu$M), **6**, and **7** ($IC_{50}$ > 1000 $\mu$M) were not active. All compounds were inactive on the activation of the alternative pathway. Two possible activation routes of the complement system are commonly referred to as the "classical" and the "alternative" activation pathway. The classical activation pathway is triggered by antibody−antigen complexes, whereas the alternative pathway can be activated by, for example, lipopolysaccharides or immune complexes that do not usually activate the classical sequence. Anticomplement activity on the classical pathway has been reported for other iridoids. For example, genipin showed 75.3 ± 1.8% inhibition at a concentration of 6.6 $\mu$M, while geniposide, geniposidic acid, and aucubin produced an inhibition of 23.0 ± 8.8, 14.3 ± 3.0, and 21.7 ± 9.7%, respectively, at a concentration of about 4 $\mu$M. After enzymatic hydrolysis with a $\beta$-glucosidase the inhibition increased up to 87.3 ± 2.3% for geniposidic acid and up to 89.3 ± 0.9% for aucubin, indicating that the hemiacetal moiety plays an important role in the anticomplementary activity of these iridoids.[12] In addition to the biologically active flavonoids reported before from the same plant, these complement-inhibiting iridoids may contribute at least in part to the complement-inhibiting properties of the crude extracts and to the traditional use against rheumatic pains.[3−6]

## Experimental Section

**General Experimental Procedures.** TLC was carried out on precoated Si gel 60 $F_{254}$ plates (Merck). Spots were detected under UV (254 and 366 nm) before and after spraying with 1% vanilin/5% $H_2SO_4$ (MeOH solutions) followed by heating the plate at 110 °C for 5 min. Preparative TLC was performed on precoated Si gel 60 $F_{254}$ plates, layer thickness 0.5 mm (Merck) unless indicated otherwise. Column chromatography was carried out on Si gel 60 (230−400 mesh, Merck) and Sephadex LH20. The semipreparative HPLC separation was performed on an apparatus consisting of the following parts: a Gilson 321 pump, a manual Rheodyne injector, a Dynamax Rainin absorbance detector model UV-1, and a recorder (type BD 111, Kipp & Zonen). Optical rotations were measured on

a Perkin-Elmer model 241 polarimeter. NMR spectra were recorded in $CD_3OD$ (99.8% D) at 30 °C on a Bruker DRX-400 instrument operating at 400 MHz for $^1H$. Chemical shifts ($\delta$) are reported in ppm downfield from tetramethylsilane (TMS), using TMS or the solvent signal as the internal standard. $^1H$, $^{13}C$ NMR, DEPT-135, and DEPT-90 (to determine carbon multiplicities) spectra were recorded, as well as two-dimensional NMR spectra: double quantum filtered (DQF) COSY to investigate $^1H-^1H$ correlations, HSQC for one-bond $^{13}C-^1H$ correlations, and HMBC for long-range $^{13}C-^1H$ correlations. The HMBC spectra were optimized for a long-range coupling constant of 8.3 Hz. Two-dimensional NMR experiments were carried out using pulsed field gradients. Mass spectra were recorded on an Autospec-oa-ToF mass spectrometer (Micromass, Manchester, UK) employing electrospray (ES) ionization. Low-energy and high-energy collision-induced dissociation (CID) spectra were acquired at a collision energy ($E_{lab}$) of 400 eV using helium or xenon, respectively, as collision gas. The collision gas was introduced into the collision cell until the $[M + Na]^+$ signal reached 60% of its original value. Accurate mass measurements were performed on the $[M - H]^-$ signal at a mass resolution of approximately 8000.

**Plant Material.** Leaves of *Morinda morindoides* (Baker) Milne-Redhead (Rubiaceae) (syn. *Gaertnera morindoides* Bak.) were collected in Kinshasa, Democratic Republic of Congo, in October 1989. The plant was identified by M. N. Nlandu of the Institut National d'Etudes et de Recherches en Agronomie (INERA) of the University of Kinshasa, where a voucher specimen (INERA 891055) is kept.

**Extraction and Isolation.** The leaves were dried at room temperature. Dried and powdered leaves (500 g) were defatted by Soxhlet extraction with *n*-hexane (2 × 1000 mL). The dried plant material was macerated and percolated exhaustively with 80% MeOH. The MeOH extract was evaporated to dryness under reduced pressure, yielding a residue of 123 g, and 50 g of it was dissolved in hot $H_2O$ (60 °C) and filtered after 24 h. The filtrate was extracted successively with $CHCl_3$ (5 × 100 mL), EtOAc (10 × 100 mL), and *n*-BuOH (10 × 100 mL).

The residue of the EtOAc fraction, after evaporation to dryness (3 g), was submitted to CC on Sephadex LH20 (70 × 4 cm) eluted with *n*-PrOH−MeOH (3:1) (1500 mL). Fractions of 20 mL were collected and analyzed by TLC developed with EtOAc−HCOOH−HOAc−$H_2O$ (30:0.8:1.2:8) (upper layer) (solvent 1). Fractions 11−18 produced colored spots after spraying and were combined. This combined fraction was further subjected to CC on Si gel (75 × 1 cm) eluted with $CHCl_3$−MeOH (3:1) (750 mL) and monitored by the same TLC system. Two major fractions were obtained and denoted fraction A (fractions 8−11) (0.23 g) and fraction B (fractions 12−27) (1.24 g). Preparative TLC of fraction A with EtOAc−MeOH (4:1) gave three bands (A1, A2, and A3). A1 was submitted to preparative TLC using solvent 1. This resulted in the isolation of white, bitter compounds **1** (15 mg, $R_f$ 0.38, solvent 1) (gaertneroside) and **2** (9.1 mg, $R_f$ 0.45, solvent 1) (acetylgaertneroside). CC on Si gel (2 × 75 cm) of fraction B using EtOAc−MeOH (4:1) as the mobile phase yielded two major fractions (B1, 0.437 g and B2, 0.368 g). CC on Si gel of fraction B1 eluted with $CHCl_3$−MeOH (3:1) (solvent 2) resulted again in the isolation of compound **2** (43 mg). CC on Sephadex LH20 of fraction B2 eluted with MeOH resulted in the isolation of a mixture of two compounds (17 mg), which were separated by semipreparative HPLC on an RP-18 LiChrosorb column (250 × 10 mm, particle size 7 $\mu$m) using a gradient from 35% to 41% MeOH in $H_2O$ in 25 min (flow rate 3 mL/min, UV detection). In this way compounds **3** (5 mg, yellowish, bitter, retention time 21.06 min; $R_f$ 0.49, solvent 1) (dehydrogaertneroside) and **4** (9 mg, yellowish, bitter, retention time 23.16 min; $R_f$ 0.41, solvent 1) (dehydromethoxygaertneroside) were obtained.

The *n*-BuOH fraction, after evaporation to dryness (2.5 g), was subjected to Sephadex LH20 (60 × 3 cm) using PrOH−MeOH (3:1) (600 mL) as the mobile phase, and fractions of 10 mL were collected and analyzed as described above. According to their chromatographic pattern, two major fractions were obtained, denoted fraction C (fractions 7−12, 1.04 g) and fraction D (fractions 13−26, 0.203 g). CC of fraction C on Si gel (75 × 2 cm), eluted with $CHCl_3$ and $CHCl_3$−MeOH (3:1), yielded 13 subfractions, among which subfractions 3 and 13 produced colored spots on TLC after spraying. Subfraction 3 (0.634 g) was submitted to CC on Sephadex LH20 eluted with EtOH (400 mL). This resulted in the isolation of compound **5** (17.6 mg, brown, bitter, $R_f$ 0.42 using *n*-BuOH−HOAc−$H_2O$ (4:1:5), upper layer) (gaertneric acid) and a mixture of compounds **1** and **6**. This mixture was separated by preparative TLC on Si gel, layer thickness 0.25 mm (Merck), using solvent 1. In this way again compound **1** (11 mg) was obtained, as well as compound **6** (white, bitter, 12 mg, $R_f$ 0.37, solvent 1) (methoxygaertneroside). CC of subfraction 13 (0.154 g) on Sephadex LH20 (75 × 1 cm) using EtOH as eluent resulted in the isolation of a mixture of two compounds (**7** and **8**), which was purified by HPLC on an RP-18 LiChrosorb column (250 × 10 mm, particle size 7 $\mu$m), using a MeCN−$H_2O$ gradient from 90% to 20% $H_2O$ in 45 min (flow rate 3 mL/min, UV detection). In this way compound **7** (white, bitter, 24 mg, $R_f$ 0.36, solvent 1) (epoxygaertneroside) and compound **8** (trace amounts, $R_f$ 0.30, solvent 1) (epoxymethoxygaertneroside) were obtained.

**Gaertneroside (1):** $[\alpha]^{25}_D$ +24.8° (*c* 0.75, MeOH); UV (MeOH) $\lambda_{max}$ 316, 298, 238 nm; $^1H$ NMR ($CD_3OD$, 400 MHz), see Table 1; $^{13}C$ NMR ($CD_3OD$, 100 MHz), see Table 1; for ES-MS and ES-MS/CID/MS, see Table 2; accurate mass measurement $[M - H]^-$ *m/z* 547.144766 (calcd for $C_{26}H_{27}O_{13}$, 547.145166) (error 0.7 ppm).

**Acetylgaertneroside (2):** $[\alpha]^{25}_D$ +23.4° (*c* 0.28, MeOH); UV (MeOH) $\lambda_{max}$ 314, 292, 234 nm; $^1H$ NMR ($CD_3OD$, 400 MHz), see Table 3; $^{13}C$ NMR ($CD_3OD$, 100 MHz), see Table 4; for ES-MS and ES-MS/CID/MS, see Table 2; accurate mass measurement $[M - H]^-$ *m/z* 589.154922 (calcd for $C_{28}H_{29}O_{14}$, 589.155731) (error 1.4 ppm).

**Dehydrogaertneroside (3):** $[\alpha]^{25}_D$ −19.5° (*c* 0.31, MeOH); UV (MeOH) $\lambda_{max}$ 291, 232 nm; $^1H$ NMR ($CD_3OD$, 400 MHz), see Table 3; $^{13}C$ NMR ($CD_3OD$, 100 MHz), see Table 4; for ES-MS and ES-MS/CID/MS, see Table 2; accurate mass measurement $[M - H]^-$ *m/z* 545.128335 (calcd for $C_{26}H_{25}O_{13}$, 545.129516) (error 2.2 ppm).

**Dehydromethoxygaertneroside (4):** $[\alpha]^{25}_D$ −15.0° (*c* 0.2, MeOH); UV (MeOH) $\lambda_{max}$ 284 nm; $^1H$ NMR ($CD_3OD$, 400 MHz), see Table 3; $^{13}C$ NMR ($CD_3OD$, 100 MHz), see Table 4; for ES-MS and ES-MS/CID/MS, see Table 2; accurate mass measurement $[M - H]^-$ *m/z* 575.139956 (calcd for $C_{27}H_{27}O_{14}$, 575.140081) (error 0.2 ppm).

**Gaertneric acid (5):** $[\alpha]^{25}_D$ +48.8 (*c* 0.21, MeOH); UV (MeOH) $\lambda_{max}$ 288, 234 nm; $^1H$ NMR ($CD_3OD$, 400 MHz), see Table 3; $^{13}C$ NMR ($CD_3OD$, 100 MHz), see Table 4; for ES-MS and ES-MS/CID/MS, see Table 2; accurate mass measurement $[M - H]^-$ *m/z* 533.129297 (calcd for $C_{25}H_{25}O_{13}$, 533.129516) (error 0.4 ppm).

**Methoxygaertneroside (6):** $[\alpha]^{25}_D$ +27.0 (*c* 0.58, MeOH); UV (MeOH) $\lambda_{max}$ 280, 222 nm; $^1H$ NMR ($CD_3OD$, 400 MHz), see Table 2; $^{13}C$ NMR ($CD_3OD$, 100 MHz), see Table 3; for ES-MS and ES-MS/CID/MS, see Table 2; accurate mass measurement $[M - H]^-$ *m/z* 577.156465 (calcd for $C_{27}H_{29}O_{14}$, 577.155731) (error 1.3 ppm).

**Epoxygaertneroside (7):** $[\alpha]^{25}_D$ +1 (*c* 0.1, MeOH); UV (MeOH) $\lambda_{max}$ 286, 224 nm; $^1H$ NMR ($CD_3OD$, 400 MHz), see Table 2; $^{13}C$ NMR ($CD_3OD$, 100 MHz), see Table 3; for ES-MS and ES-MS/CID/MS, see Table 2; accurate mass measurement $[M - H]^-$ *m/z* 563.139783 (calcd for $C_{26}H_{27}O_{14}$, 563.140081) (error 0.5 ppm).

**Epoxymethoxygaertneroside (8):** $^1H$ NMR ($CD_3OD$, 400 MHz), see Table 2; $^{13}C$ NMR ($CD_3OD$, 100 MHz), see Table 3; for ES-MS and ES-MS/CID/MS, see Table 2; accurate mass measurement $[M - H]^-$ *m/z* 593.149487 (calcd for $C_{27}H_{29}O_{15}$, 593.150646) (error 2.0 ppm).

**Anticomplementary Activity.** The complement modulation test applied was based on the assay models as described by Mayer[13] and by Platts-Mills and Ishizaka[14] for the classical

and the alternative pathway, respectively. It was adapted for use on a microscale by Klerx et al.[15] as described before.[16] Dose−response curves were obtained using seven different concentrations of the test sample, and the $IC_{50}$ value determined. Results are presented as $IC_{50} \pm$ SD (standard deviation) calculated from two or three independent measurements. Dextrane sulfate, with an average molecular weight of 500 000, was used as the positive control,[17] producing an $IC_{50}$ of 0.19 ± 0.05 nM.

**Acknowledgment.** Financial support from the Fund for Scientific Research (FWO−Flanders, Belgium) (project number G.0082.98; fellowship for S.A.) and from the Special Fund for Research of the University of Antwerp is gratefully acknowledged.

## References and Notes

(1) Kambu, K. *Eléments de Phytothérapie Comparée. Plantes Médicinales Africaines*; CRP: Kinshasa, 1990.
(2) Kerharo, J.; Adam, J. G. *La Pharmacopée Sénégalaise Traditionnelle. Plantes Médicinales et Toxiques*; Vigot et Frères: Paris, 1974
(3) Cimanga, K.; De Bruyne, T.; Lasure, A.; Li, Q.; Pieters, L.; Claeys, M.; Vanden Berghe, D.; Kambu, K.; Tona, L.; Vlietinck, A. J. *Phytochemistry* **1995**, *38*, 1301−1303.
(4) Cimanga, K.; De Bruyne, T.; Lasure, A.; Van Poel, B.; Vanden Berghe, D.; Kambu, K.; Tona, L.; Vlietinck, A. J. *J. Nat. Prod.* **1995**, *58*, 372−378.
(5) Cimanga, K.; De Bruyne, T.; Van Poel, B.; Ma, Y.; Claeys, M.; Pieters, L.; Kambu, K.; Tona, L.; Bakana, P.; Vanden Berghe, D.; Vlietinck, A. J. *Planta Med.* **1997**, *63*, 220−223..
(6) Cimanga, K.; De Bruyne, T.; Hu, J. P.; Cos, P.; Apers, S.; Pieters, L.; Tona, L.; Kambu, K.; Vanden Berghe, D.; Vlietinck, A. J. *Pharm. Pharmacol. Commun.* **1999**, *5*, 419−424.
(7) Boros, C. A.; Stermitz, F. R. *J. Nat. Prod.* **1991**, *54*, 1173−1246.
(8) Abe, F.; Mori. T.; Yamauchi, T. *Chem. Pharm. Bull.* **1984**, *32*, 2947−2956.
(9) Adegosan E. *Phytochemistry* **1979**, *18*, 175−176.
(10) Sang, S.; Cheng, X.; Zhu, N.; Wang, M.; Jhoo, J.; Stark, R. E.; Badmaev, V.; Ghai, G.; Rosen, R. T.; Ho, C. *J. Nat. Prod.* **2001**, *64*, 799−800.
(11) Kanchanapoom, T.; Kasai, R.; Yamasaki, K. *Phytochemistry* **2002**, *59*, 551−556.
(12) Oshima, Y.; Takata, S.; Hikino, H.; Deyama, T.; Kinoshita, G. *J. Ethnopharmacol.* **1988**, *23*, 159−164.
(13) Mayer, M. M. In *Experimental Immunochemistry*; Kabat, E. A., Mayer, M. M., Eds.; Thomas: Springfield, IL, 1971; pp 133−240.
(14) Platts-Mills, T.; Ishizaka, K. *J. Immunol.* **1974**, *113*, 348−358.
(15) Klerx, J. P. A. M.; Beukelman, C. J.; Van Dijk, H.; Willers, J. M. N. *J. Immunol. Methods* **1983**, *63*, 215−220.
(16) Huang, Y.; De Bruyne, T.; Apers, S.; Ma, Y.; Claeys, M.; Vanden Berghe, D.; Pieters, L.; Vlietinck, A. *J. Nat. Prod.* **1998**, *61*, 757−761.
(17) Wuillemin, W. A.; te Velthuis, H.; Lubbers, Y. T. P.; de Ruig, C. P.; Eldering, E.; Hack, C. E. *J. Immunol.* **1997**, *159*, 1953−1960.

NP020215H